Bulgarian Journal of Meteorology and Hydrology

Национален институт по метеорология и хидрология

National Institute of Meteorology and Hydrology

Bul. J. Meteo & Hydro 27/2 (2023)

Study on the spatial pattern of black carbon in Sofia

Elena Hristova*, Georgi Tsekov, Blagorodka Veleva, Valeri Nikolov

National Institute of Meteorology and Hydrology,
Tsarigradsko shose 66, 1784 Sofia, Bulgaria

Abstract: Air pollution with particulate matter (PM) is still a big problem in the large urban agglomerations in the world as well as in most of the cities of Bulgaria. The urban air quality is determined by a variety of factors: air masses, characteristic local flow and meteorology, low dispersion ability in built-up environments, concentration of emission sources of different types, chemical processes. The PM toxic effect is not only due to its size but also to their chemical composition. The PM chemical composition, thus, reflects site specific complex processes. Black Carbon (BC) is one of the components of the PM that affects both human health and contributes to climate change. It is emitted by the incomplete combustion of fossil fuels, biofuels and biomass. This work presents the study on the spatial pattern of black carbon (BC) at a high spatial resolution in the districts "Pavlovo", "Buxton" and "Manastirski livadi" in Sofia. Along with BC concentrations, the data for hourly concentrations of PM_{10}, NO_2, SO_2, CO measured at AMS "Pavlovo", ExEA and the meteorological parameters, including temperature, relative humidity, and wind speed conditions are presented and discussed. The BC concentrations showed significant spatial heterogeneity and variations peaking in the morning. The highest concentrations of BC were observed near roadways with heavy traffic.

Keywords: $PM_{2.5}$, Black carbon, MA200, air pollution

1. INTRODUCTION

The problem with air quality in the city of Sofia is related to the presence of a high number of motor vehicles, industrial and domestic heating sources. The city is placed in a semi-closed valley where unfavourable meteorological conditions, in particular in cold periods of the year, are observed. The well-recognized important pollutants like fine dust particles with an aerodynamic diameter (AD) less than 10 microns (μm, PM_{10}), those with AD less than 2.5 μm ($PM_{2.5}$), polycyclic aromatic hydrocarbons (PAHs),

* elena.hristova@meteo.bg

NO_2, benzene, SO_2, O_3 are measured continuously at automatic measuring stations (AMS). Unfortunately, information about other pollutants of emerging concern like BC (Black carbon, Organic carbon, Elemental carbon) is limited. They are not considered in a "Comprehensive Program for Improving Atmospheric Air Quality on the territory of Sofia Municipality for the Period 2021-2026" (PIAQ2021).

The first information for BC concentrations in Bulgaria (Hristova et al., 2020, 2022) has been obtained in the frame of the projects IAEA TC RER7012 and "CARBOAEROSOL" (a project funded by Bulgarian Science Fund (КП-06-Н34/9_19.12.2019)).

Carbonaceous particles or so called black carbon – BC are an important component of the atmospheric aerosol and usually for the region of Europe they make up 20 -45% mass concentration of $PM_{2.5}$ and 20 -30% air particulate fraction PM10 (Putaud et al. 2010; Ytri et al., 2007; Gerlos-Nijland et al., 2012). The study of carbon particles in urban areas is of great importance in determining the contribution of transport and domestic heating to air pollution. Different terms for carbon particles can be found in the scientific literature: light absorbing carbon (LAC), black carbon (BC), brown carbon (BrC), elemental carbon (EC) and organic carbon (OC). There is no generally accepted definition of the term "Black carbon". Correct term for BC following Petzold, 2013 should be "Mixed particles containing a BC fraction should belter named BC-containing particles instead of BC particles or soot particles".

Sometimes the term equivalent Black carbon (eBC) is used instead of black carbon for data derived by optical absorption methods, together with a suitable mass absorption cross-section (MAC) for the conversion of light absorption coefficient into mass concentration.

The measurement of BC in particles is based mainly on light absorption or optical properties of BC while the measurements of EC and OC is usually monitored with thermal-optical methods (Cavalli et al., 2011). However, the average values of BC and EC in urban conditions obtained by different methods are comparable (Hutzenberger et al., 2006; Slowik et al., 2007). Black carbon is associated with serious impacts on climate and human health (Ytri et al., 2007; Gerlos-Nijland et al., 2012; Hutzenberger et al., 2006; Slowik et al., 2007; IPCC, 2013; WHO, 2021).

BC is formed by the incomplete combustion of fossil fuels, biomass and biofuels. Fine particulate carbonaceous particle contains not only elemental carbon but also includes toxic and carcinogenic substances (PAHs for example) (Bond T. C, 2013; Bessagnet and Allemand, 2020). BC is directly emitted into the air unlike some pollutants which are formed in the atmosphere from precursors. Major sources include vehicles (particularly diesel-driven road vehicles), non-road mobile machinery, ships, residential heating (e.g. small coal or wood burning stoves) and open biomass burning (e.g. forest fires or burning of agricultural waste). BC can stay in the atmosphere for days and weeks (Gerlos-Nijland et al., 2012).

BC is more often associated with small aerosol particles which can penetrate deeply into the human respiratory system. BC could be particularly useful to evaluate not only the health risks of air pollution dominated by primary combustion emissions but also the benefits of traffic abatement measures. This is the reason to be chosen as pollutant in this experimental study. When it is measured in not heating season its main source is the traffic. In the European Environment Agency (EEA) Technical report No 18/2013 the importance of monitoring of the black carbon as a proxy for traffic combustion exhaust is underlined.

The emissions of BC can be estimated by emission inventories. It is included in the official EMEP/EEA air pollutant emission inventory guidebook, 2019. There is some uncertainty in this means of estimating BC emissions, but the advantage is that the BC fraction is consistent with the $PM_{2.5}$ fraction.

Sources of BC can vary greatly in different regions of the world. The main sources in Europe are diesel road and off-road vehicles, shipping and the burning of various heating fuels. In general higher BC concentrations are observed in the cold period of the year, mainly because of the higher emissions from heating and unfavorable meteorological conditions. In summer due to the dry and hot weather forest fires can contribute significantly for elevated BC (as brown carbon from biomass burning – BrC) concentrations (Bessagnet and Allemand, 2020; Kunder et al., 2018; Ziola et al., 2021; Diapouli et al., 2017; Helin et al., 2018; Beekmann et al., 2015; Becerril-Valle et al., 2017; Kucbel et al., 2017; Bernaedoni et al., 2021).

This work is focused on the experimental study of spatial and temporal variations of Black carbon concentration in the districts “Pavlovo”, “Buxton” and “Manastirski livadi” in Sofia and their relationship with road traffic.

2. METHODOLOGY

2.1. The study area

The study area is in the districts “Pavlovo”, “Buxton” and “Manastirski livadi” (see Figure 1). The routes were carried out on the right side of the road due to people's daily habits (driving and walking on the right side in Bulgaria). All walks along the route were conducted on weekdays (5 Oct 2021, 29 June 2022 and 19 Oct 2022), with clear skies, with no precipitation, calm winds, in warm part of the year (non-heating season) to avoid misrepresentation of typical urban air exposure conditions from the traffic. The route started from the Square „Zname na mira” and continued approximately 4.5 km for 1 h with average walking time, passing through different types of streets (roads with high traffic and small streets with less traffic) to avoid misrepresentation of typical urban air exposure conditions and to track the influence of traffic on BC concentrations.

Fig. 1. Map with tracking route in the studied area

2.2. Measurement of short-term BC concentrations in the air

The main instrument used for BC measurements in the current study is microAeth® MA200 (MA200; AethLabs, San Francisco, CA, USA). The MA200 instrument makes real-time five wavelength optical analyses by measuring the rate of decrease in transmitted light through the sample filter, due to continuous particle deposition on the filter. The 5 analytical channels are measuring at 880 nm, 625 nm, 528 nm, 470 nm, 375 nm wave lengths. Measurement at 880 nm is interpreted as the concentration of Black Carbon (BC). The MA200 includes miniature cartridges that have a reel of filter tape for particle collection and on-board analysis. The tool automatically controls the movement of the tape, moving to a new unused location. This way the instrument can work continuously for several weeks or months without technical human intervention. The microCyclone $PM_{2.5}$ Size-selective inlet is used to provide a $PM_{2.5}$ size cut point to a 50 ml/min flow rate. The microAeth has access to the Global Positioning System with a built-in antenna. The GPS is used for precise, automatic time synchronization and for optional location tracking. The detection limit is 30 ng/m^3 and the measurement resolution 1 ng/m^3 (aethlabs.com). The measurement settings conducting in this study were: sampling airflow - 50 ml/min, integration measurement time – 60 sec, in Single Spot mode.

2.3. Comparison with other air pollutants

To compare our measured concentrations of BC with other major air pollutants, data for hourly concentrations of PM_{10}, NO_2, SO_2, CO measured at AMS “Pavlovo” of the

Executive Environment Agency (ExEA) for the dates of all field campaigns are used. “Pavlovo” station is chosen as it is the nearest one to the districts “Pavlovo”, “Buxton” and “Manastirski livadi”.

2.4. Characteristics of meteorological conditions

The analysis of the synoptic situation for the days of the measurements is based on data for main meteorological elements/parameters from both observation and a model. The meteorological data were obtained from the regular observations at the central meteorological observatory of the NIMH in Sofia, which is located in “Mladost 1A” district. The indicated temperature at 850 hPa level is taken from the data obtained from the regular NIMH vertical aerological soundings at 06 UTC and 12 UTC. The measurements are made with instruments certified by the World Meteorological Organization and are regularly calibrated. The measurement data are fed into the international meteorological data exchange and are official for the country. Although the location of the meteorological measurements does not fully coincide with the study area, the measured meteorological elements in the specific synoptic settings are relevant for the whole city and are sufficiently reliable and relevant for the assessment of the air pollution potential in Sofia.

To assess the spatial distribution of the meteorological fields, simulations were run with the WRF regional numerical weather model using the Advanced Research WRF (ARW) dynamical kernel, version 3.5.1, for all field measuring campaigns. The ARW, developed by the Mesoscale and Microscale Meteorology Division of NCAR and community, is designed to be a flexible, state-of-the-art atmospheric simulation system that is portable and efficient on available parallel computing platforms. The ARW is suitable for use in a broad range of applications across scales ranging from meters to thousands of kilometers. The WRF modeling system software is in the public domain and is freely available for community use.

The initial and boundary conditions are the results of the Global Forecast System (GFS), the weather forecast model of the US NCEP, which are freely available for general use via the Internet. The model was run on three nested computation regions with a spatial resolution of 25, 5 and 1 km and 38 vertical levels, respectively. The used parameterizations schemes are given in Table 1. The model output was processed with NCL-NCARG to visualize the meteorological fields of interest. The results are presented in the next section of this manuscript as figures with the spatial distributions of the temperature, relative humidity and wind fields at ground and altitude (here dew point temperature instead of relative humidity).

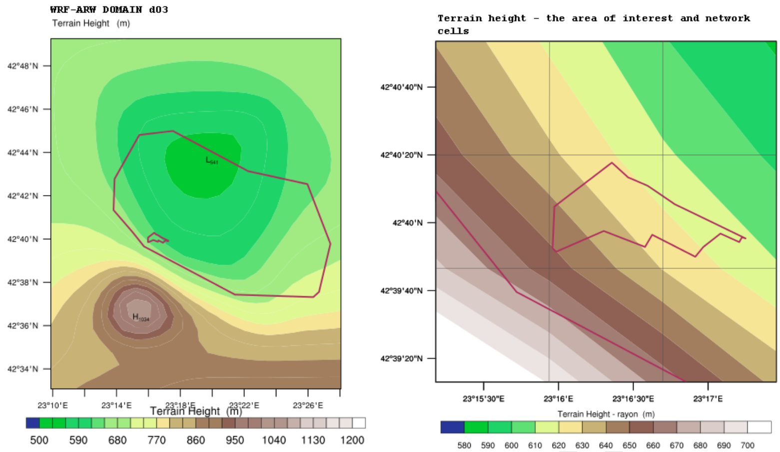

Fig. 2. Terrain height in the simulation region (left) and in the part of it covering our region of interest (right) (The solid lines in chestnut color indicate the boundaries of Sofia on the ring road and the experiment area)

Table 1. The parameterization schemes of the Advanced Research WRF

Microphysics	Eta microphysics: The operational microphysics in NCEP models. A simple efficient scheme with diagnostic mixed-phase processes. (Phis opt=5)
Cumulus Parameterization	Grell-Devenyi (GD) ensemble scheme: Multi-closure, multi-parameter, ensemble method with typically 144 sub-grid members (Cu opt = 3)
Planetary Boundary layer	Mellor-Yamada-Janjic scheme: Eta operational scheme. One-dimensional prognostic turbulent kinetic energy scheme with local vertical mixing (PBL opt = 2). 2d Deformation: K for horizontal diffusion is diagnosed from just horizontal deformation. The vertical diffusion is assumed to be done by the PBL scheme
Longwave Radiation	RRTM scheme (ra_lw_physics = 1): Rapid Radiative Transfer Model. An accurate scheme using look-up tables for efficiency. Accounts for multiple bands, and microphysics species. For trace gases, the volume-mixing ratio values for CO_2 =379e-6, N_2O=319e-9 and CH_4=1774e-9.
Shortwave Radiation	RRTMG shortwave scheme with the MCICA method of random cloud overlap.
Surface Layer	Eta similarity: Used in Eta model. Based on Monin-Obukhov with Zilitinkevich thermal roughness length and standard similarity functions from look-up tables

Land Surface	5-layer thermal diffusion: Soil temperature only scheme, using five layers
Urban Surface	Urban canopy model (1): 3-category UCM option with surface effects for roofs, walls, and streets.

3. RESULTS AND DISCUSSION

3.1. Spatial and temporal variations of BC concentrations during field campaigns

Three BC measuring campaigns have been carried out - one in summer (2022) and two in the autumn (2021 and 2022) – at three time intervals: rush hours in the morning (8:30 – 9:45h), midday (12:30 – 14:00h) and at late afternoon (17:00 – 18:30h). The time variations of BC concentrations during all field measuring campaigns are illustrated in Figure 3. Hot spots with maximum measured BC concentration are marked on the map presented as Figure 4. The measured BC concentrations are ranged from 1 to 48.8 μg/m^3. As it was expected, the higher BC concentrations were measured in the morning for all field experiments compared to those measured in the midday and late afternoon. The areas with highest traffic intensities, particularly on crossroads, showed high BC concentrations. An example of the BC concentration variation along the measurement path on 19 Oct 2022 at time slot 8:30 – 9:30 is illustrated in Figure 5.

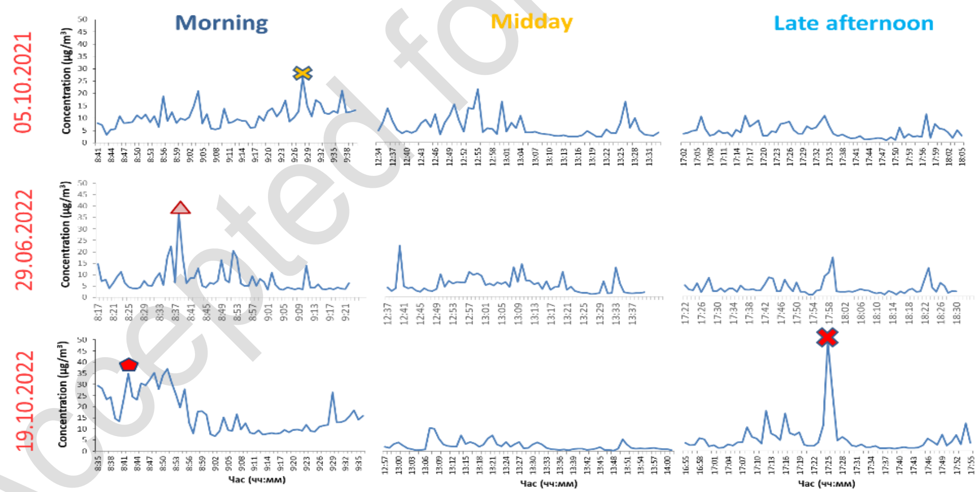

Fig. 3. The time variations of BC concentrations on 5 Oct 2021, 29 Jun 2022 and 19 Oct 2022

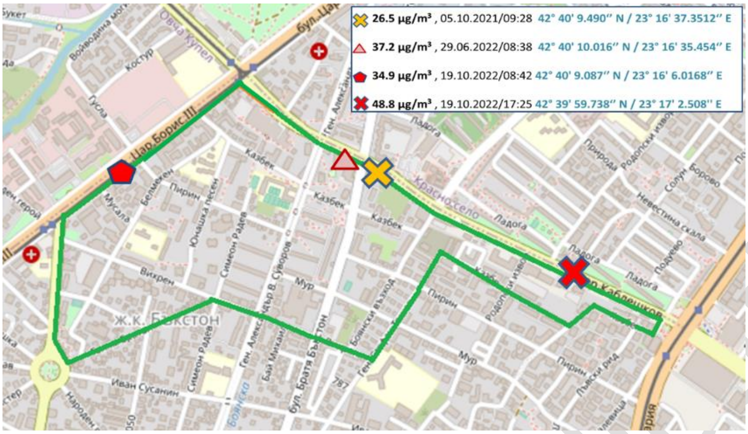

Fig. 4. Map with the tracking route and hot spots with maximum measured BC concentration

As seen in Figure 5, the highest values (25 -38 μg/m^3) in the morning hours are observed on the most heavily trafficked roads: Blvd. "Tsar Boris III" and "Todor Kableshkov" Street. It is worth noting that the BC concentrations in the small streets inside the residential district are 2-3 times less than those along the two big boulevards. A maximum of all measured values is registered in the traffic jam before the "Todor Kableshkov" connection to the blvd "Bulgaria" when diesel trucks and engines were blocked before the intersection, Figure 4. The average concentration for all measurement campaigns varies from 3.7 (29 Jun 2022, midday) to 16.8 μg/m3 (19 Oct 2022, late afternoon).

Fig. 5. An example of the BC concentration variation along the measurement path on 19 Oct 2022 at time slot 8:30 – 9:30

The diurnal pattern of major pollutants PM_{10}, NO_2, SO_2, CO measured at AMS "Pavlovo", were examined for all days of the experiment. The diurnal concentration variation of these pollutants together with the mean BC concentrations obtained during the measurement campaigns on 5 Oct 2021, 29 Jun 2022 and 19 Oct 2022 are presented in Figure 6.

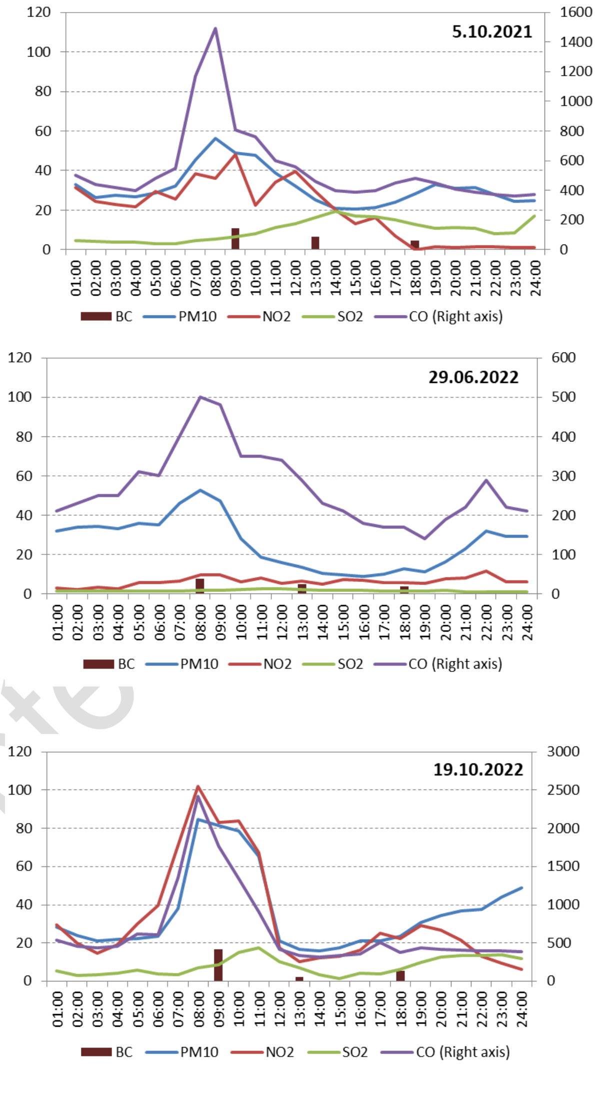

Fig. 6. Diurnal pattern of major pollutants PM_{10}, NO_2, SO_2, CO measured at AMS "Pavlovo" (lines) and mean BC concentration (bars) on 5 Oct 2021, 29 Jun 2022 and 19 Oct 2022

It can be clearly seen that in the time slot 7:00 – 11:00 h, when the traffic is intense and the turbulent mixing in the developing ABL is limited, the concentrations of all pollutants, as well as of the measured BC values are higher than in mid-day hours. The evolution of the Mixing layer height were obtained from the regular NIMH vertical aerological soundings at 6 UTC and 12 UTC (Figure 8, 11, 14) and from WRF modelling data (Figures 10, 13, 16). For example, the vertical profiles for 5 Oct 2021 show a change from about 100 m at 6 UTC to > 400 m at 14 UTC (Figure 8 and 10). Late in the afternoon, when the traffic is intensified but the mixing layer high is close to the daily maximum, slight increase in concentrations of all pollutants is observed.

The summary statistics are given in Table 2. Minimum concentrations of BC and SO_2 are approximately 1 μg/m^3, for NO_2 even lower, 0.1 μg/m^3. The minimum of CO is about parts of mg/m^3. All traffic related pollutants BC, PM_{10}, NO_2 and CO show maximum values on 19 Oct 2022. A strong correlation was also obtained for NO_2 and CO (0.89) on that day.

Table 2. Statistical parameter as min, max and mean values

Date	μg/m^3	BC_8h	BC_13h	BC_18h	PM_{10}	NO_2	SO_2	CO
5.10.2021	min	3.3	2.4	1.0	20.4	0.1	3.2	360.0
	max	26.5	21.8	11.4	56.5	48.3	19.2	1490.0
	mean	11.0	6.5	4.5	31.5	19.5	9.9	546.3
26.06.2022	min	3.4	1.1	0.8	8.8	2.4	1.1	140.0
	max	37.2	21.6	17.3	52.6	11.7	2.8	500.0
	mean	7.8	5.1	3.7	25.8	6.3	1.7	270.4
19.10.2022	min	6.8	0.2	1.1	15.9	6.2	1.6	320.0
	max	37.0	10.5	48.8	84.7	102.1	7.5	2420.0
	mean	16.8	2.4	5.5	35.7	32.6	7.9	668.3

3.2. Synoptic conditions

In this section are presented the synoptic conditions for all three days of the experiments based on observations in Central Meteorological Observatory (CMO) at the National Institute of Meteorology and Hydrology (NIMH) and modelled data from the WRF model.

During the three days of the field experiment it was almost calm, with light winds mainly in the afternoon. As it was forecasted, there was no precipitation. There was a near-surface retentive layer (temperature inversion) in the morning hours, which broke down during the days that led to improved vertical mixing conditions.

On **5th of October 2021**, the country is situated in an area of high atmospheric pressure with small horizontal gradient. At a 500 hPa isobaric level, the weather is defined by a well expressed baric ridge with a distinctly warm air mass. The air flow at level 850 hPa is weak from the south-southwest and warmer air penetrates with it. The weather is sunny, almost calm before midday, with breezes from the eastern quarter after midday. In the morning hours, the atmospheric boundary layer is stably stratified and there is a surface temperature inversion. According to the NIMH's aerological sounding from 06 UTC (Figure 8) its upper boundary is at altitude of about 1000 m a.s.l. or 380-400 m a.g.l., above which the temperature profile is neutral. The lack of turbulence and atmospheric dynamics favours the retention of atmospheric pollutants in the ground layer. During the daytime, as the surface temperature increases, the surface temperature inversion breaks down and the conditions for convection improve, thereby increasing turbulence. The occurrence of weak winds further aids the pollutant dispersion process.

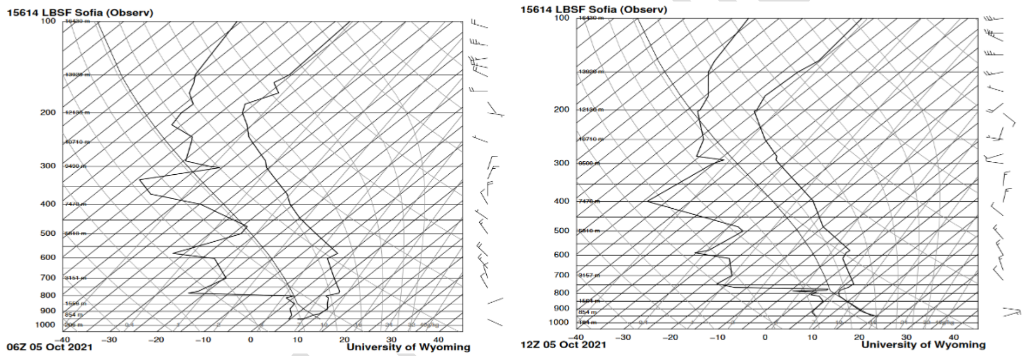

Fig.8 NIMH's aerological sounding data from 06 UTC (left) and 12 UTC (right) on 5 Oct 2021

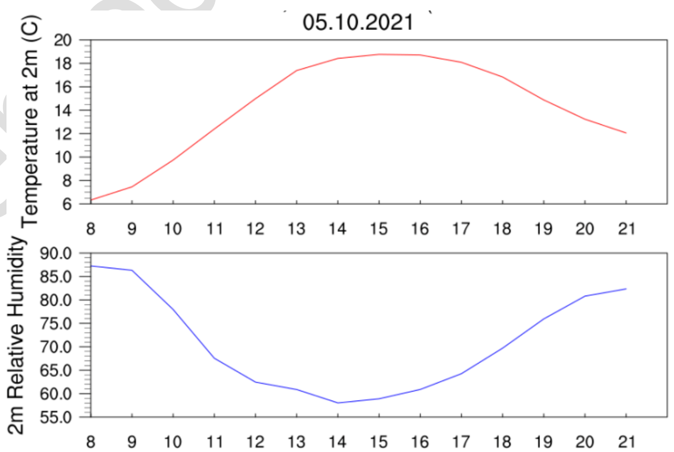

Fig. 9. Temperature and relative humidity on 5 Oct 2021 at a central point of the experiment area: lat=42.6678, lon=23.2768, local time -LT (+3UTC) from WRF model

As it's seen in the figures above (Figure 9) from the WRF model, the values of the temperature and humidity follow the expected diurnal evolution for the synoptic conditions and orographic features. The most moistly, cold and calm weather in the study area is in the morning, but at this time the humidity over the Vitosha Mountain decreases. In the midday, the weather in the study area is significantly warmer and least humid. In the late afternoon the temperature slightly increases, the humidity rises and the wind velocity is higher. The height of the morning inversion area is computed to be around 100 m a.g.l. In the layer between 100 and 400 m, the temperature decreases with altitude and above 400 m there is an isothermal layer up to 800 m (Figure 10).

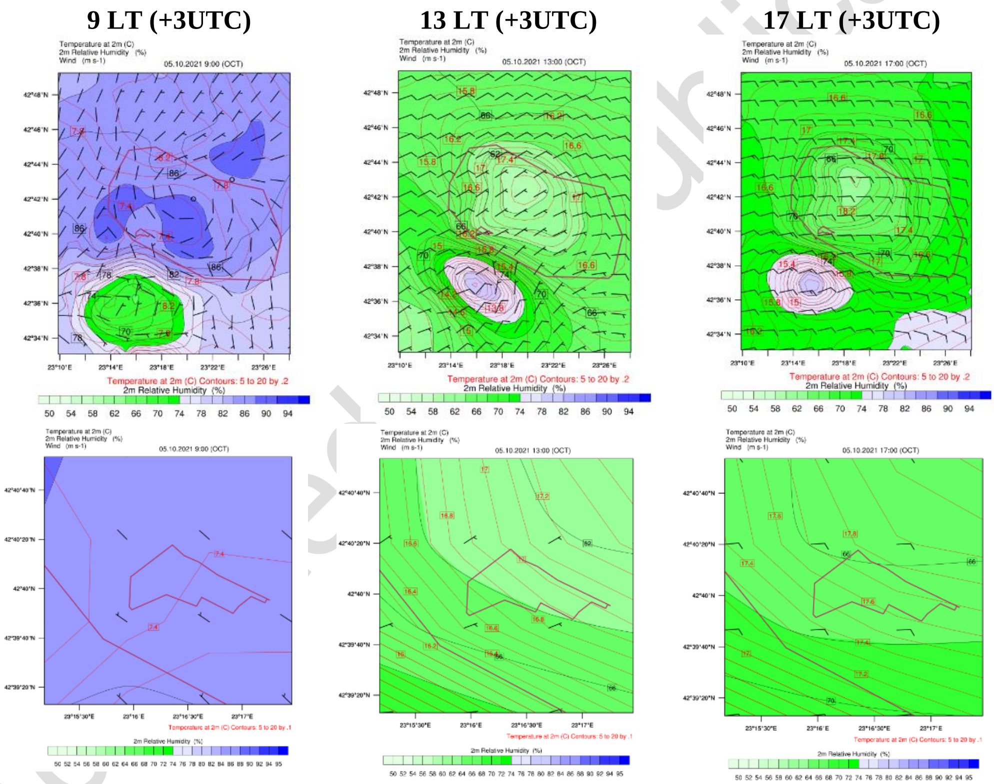

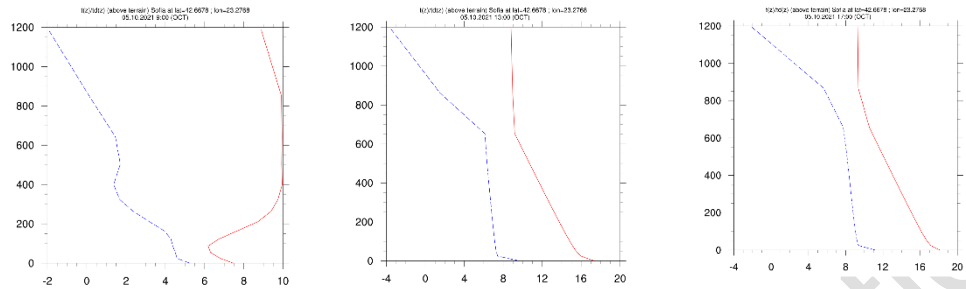

Fig.10. Temperature (red contour lines) and relative humidity (filled contours) fields at 2 m and wind vectors at 10 m above the ground surface, and vertical profile of temperature and dew point at a central point of the studied area for 09, 13, 17 h local time (LT)

29th of June 2022: Western Bulgaria is under the influence of a 500 hPa isobaric ridge with an axis passing through the western Balkan Peninsula and southern Italy. Air flow at isobaric level 850 hPa is weak from east-northeast. The horizontal pressure gradient is weak and the pressure value is close to the average for June. During the daytime it decreases by about 2.5 hPa. The weather is sunny, daytime temperatures are rising. Calm weather prevails with insignificant and temporarily light winds from the north-northeast. In the morning, there is a thin inversion layer (Figure 11) which quickly dissipates, and there is a weak convection, which favours faster dissipation of pollutants in the ground layer.

The actual weather conditions are well reproduced by the WRF model results (Figure12). It is cold and humid in the morning and it becomes warmer, drier and windier in the afternoon. The vertical temperature profile is normal, except in the morning when there is a lifted inversion layer between 200 and 400m a.g.l. (Figure 13).

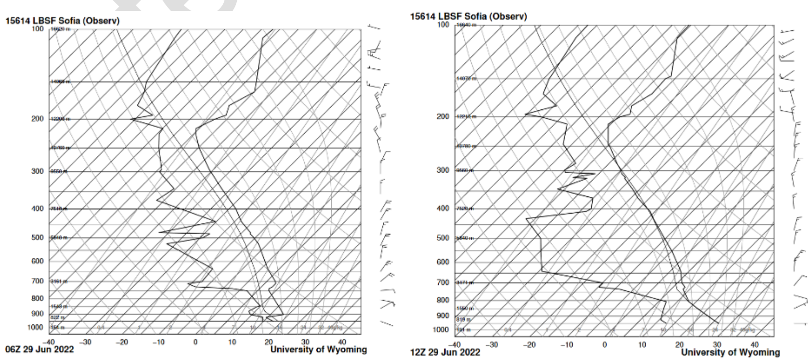

Fig.11. NIMH's aerological sounding data from 06 UTC (left) and 12 UTC (right) on 29 June 2022

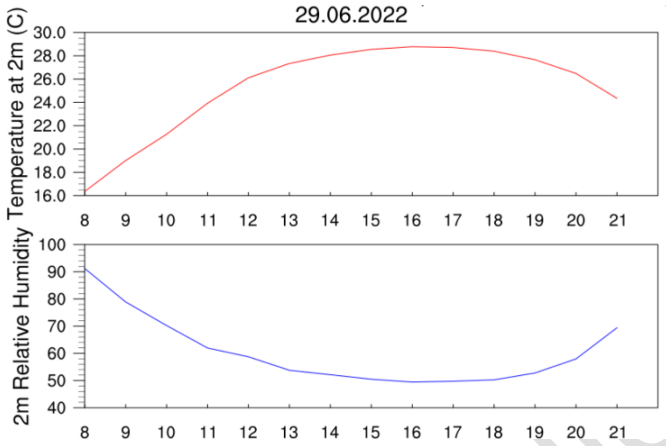

Fig. 12. Temperature and relative humidity on 29 Jun 2022 at a central point of the studied area: lat=42.6678, lon=23.2768, LT (+3UTC) from WRF model

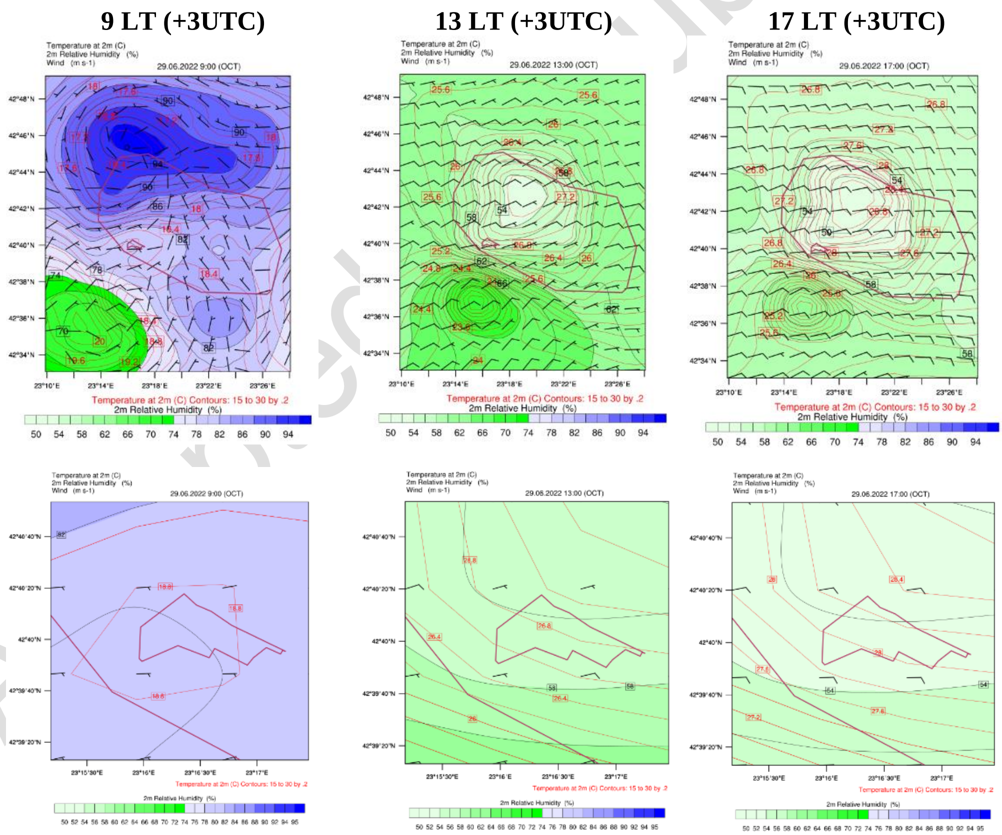

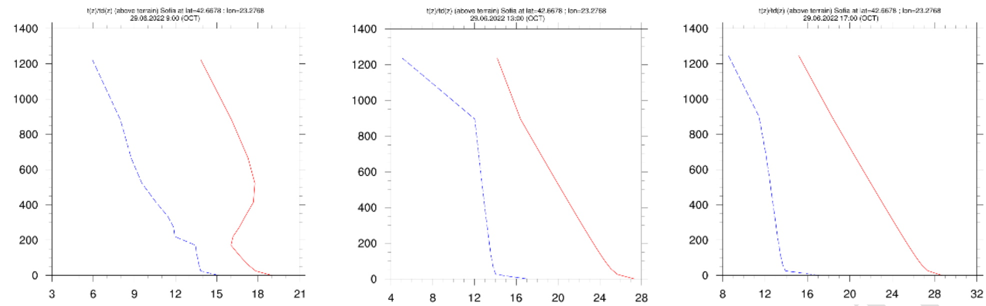

Fig. 13. Temperature (red contour lines) and relative humidity (filled contours) fields at 2 m; wind vectors at 10 m above the ground surface and vertical profile of temperature and dew point at a central point of the studied area for 09, 13, 17 h LT (+3UTC)

On 19th of October 2022, a temporary disruption of the 500 hPa level baric ridge is observed, under influence of a baric valley descending from the north. The air flow at the 850 hPa level is weak from the northwest and colder air penetrates with it. The influence of the surface anticyclone over Eastern Europe is weakening, lowering the surface pressure by about 4 hPa during daylight hours. This does not change the prevailing sunny weather. It is almost calm or with very weak wind in the morning from the southern quarter; in the afternoon the wind slightly increases its velocity and turns from the west.

In the morning there is a temperature inversion layer up to about 1000 meters a.s.l. (380-400 m a.g.l.), and up to about 2500 meters the temperature profile is isothermal. During the day, as the temperature rises, the inversion layer breaks down (Figure 14). The isothermal layer aloft is broken with a penetration of colder air at altitude and, at the end of the day, the vertical temperature profile becomes neutrally stratified. The increasing wind velocity, atmospheric dynamics and turbulence lead to improved conditions for pollutants dispersion.

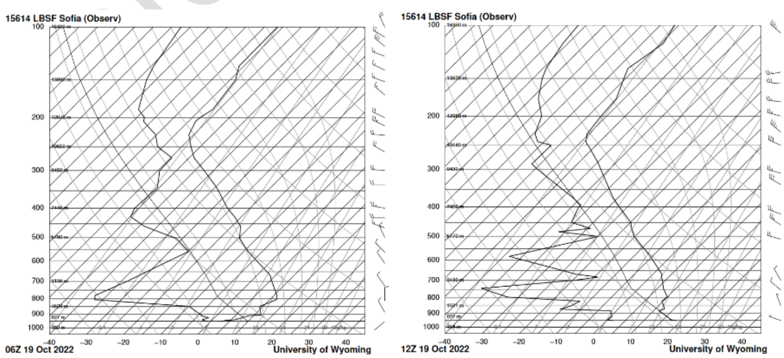

Fig.14. NIMH's aerological sounding data from 06 UTC (left) and 12 UTC (right) on 19 Oct 2022

The diurnal dynamics of meteorological elements temperature and humidity are well reproduced by the WRF model: moistly and cold morning, warm and relatively dry midday and relatively warm afternoon with rising humidity and weak western wind (Figure 15). At 09 h LT the temperature inversion is computed and visualized in the layer from 0 to 600 m. The destruction of the inversion and the restoration of the normal vertical temperature profile are visible in the next two graphs at 13 and 17 h LT, Figure 16.

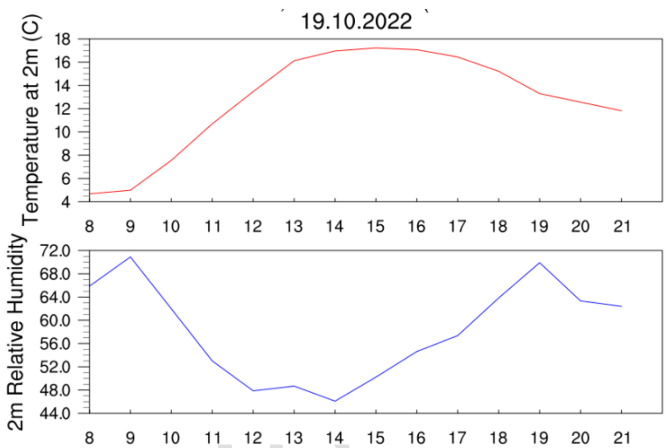

Fig 15. Temperature and relative humidity during the day on 19 Oct 2022 at a central point of the studied area: lat=42.6678, lon=23.2768, LT (+3UTC) from WRF model

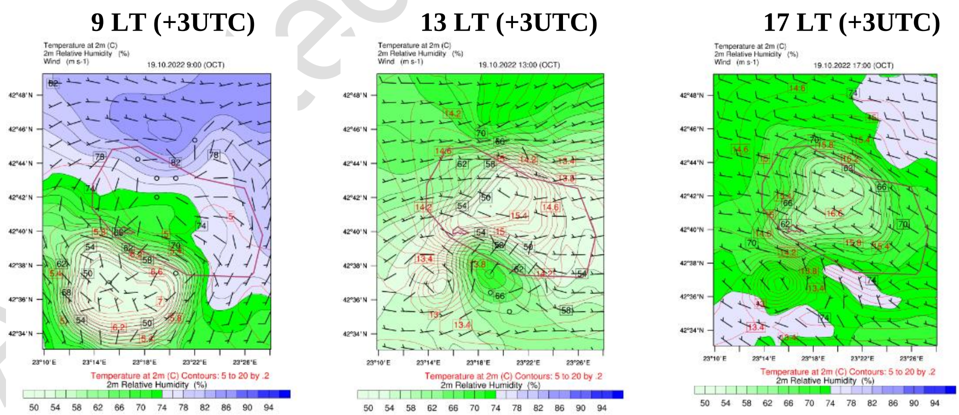

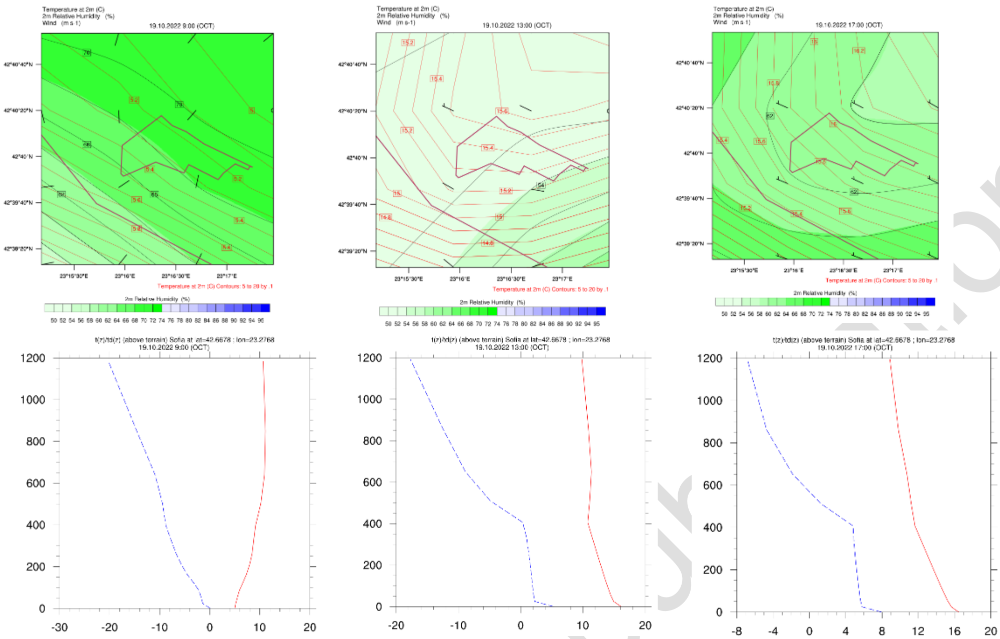

Fig. 16. Distribution of temperature (red contour lines) and relative humidity (filled contours) at 2 m and wind vectors at 10 m above the ground surface (left and middle) and vertical profile of temperature and dew point at a central point of the studied area at 09, 13, 17 h LT (+3UTC)

4. CONCLUSIONS

The experimental study of spatial and temporal variations of Black carbon concentration related to road traffic in the districts “Pavlovo”, “Buxton” and “Manastirski livadi” has been done. The approach for mobile measurements of BC with portable aethalometer is proved to reflect the Black carbon emissions of the traffic origin and the traffic intensity itself. The time variation of BC corresponds to the variations of other traffic dependent pollutants as NO_2, PM_{10}, CO, measured at the stationary AMS of ExEA “Pavlovo” situated close to the studied area. The meteorological conditions, viewed as synoptic situations, modeled by the WRF system and evaluated on the basis of actually measured meteorological parameters – temperature inversions, dynamic mixing due to the wind, etc. – show the role of atmospheric conditions for dispersion of impurities, in particular, on the average values of the measured concentrations of BC. The extreme maximum in a similar meteorological situation, not changing sufficiently during a period of 1-1.5 hour, is result of the traffic intensity, traffic jams and specific impact from old diesel engines which are able to increase the concentration several times in the frame of the tens or hundreds of meters and in short time intervals.

ACKNOWLEDGEMENTS

This study was performed in the frame of and with the financial support of INNOAIR "Innovative demand responsive green public transportation for cleaner air in urban environment" -UIA05-202 and with technical support by project "CARBOAEROSOL" supported from the Bulgarian National Science Fund trough contract № КП-06-Н 34/9 -19.12.2019. The authors also acknowledge the ExEA for the air pollutants data provided.

REFERENCES

Bernardoni, V., Ferrero, L., Bolzacchini, E., Forello, A. C., Gregorič, A., Massabò, D., Močnik, G., Prati, P., Rigler, M., Santagostini, L., Soldan, F., Valentini, S., Valli, G., Vecchi, R. (2021), Determination of Aethalometer multiple-scattering enhancement parameters and impact on source apportionment during the winter 2017/18 EMEP/ACTRIS/COLOSSAL campaign in Milan, Atmos. Meas. Tech., 14, 2919–2940, https://doi.org/10.5194/amt-14-2919-2021.

Becerril-Valle, M., Coz, E., Prévôt, A.S.H., Moˇcnik, G., Pandis, S.N., Sánchez de la Campa, A.M., Alastuey, A., Díaz, E., Pérez, R.M., Artíñano, B. (2017), Characterization of atmospheric black carbon and co-pollutants in urban and rural areas of Spain. Atmos. Environ. 169, 36–53.

Beekmann, M., Prévôt, A.S.H., Drewnick, F., Sciare, J., Pandis, S.N., Denier van der Gon, H.A.C., Crippa, M., Freutel, F., Poulain, L., Ghersi, V.; et al. (2015), In Situ, satellite measurement and model evidence on the dominant regional contribution to fine particulate matter levels in the Paris megacity. Atmos. Chem. Phys., 15, 9577–9591.

Bessagnet B., Allemand N. (2020), Review on Black Carbon (BC) and Polycyclic Aromatic Hydrocarbons (PAHs) emission reductions induced by PM emission abatement techniques, TFTEI Techno-Scientific Secretariat, Paris, France, pp. 156.

Bond T. C, et al., (2013), Bounding the role of black carbon in the climate system: A scientific assessment, JGA Atmospheres, Vol. 118, 11, 5380-5552

Cavalli, F., Viana, M., Espen, K., Kiss, G., Genberg, J. and Putaud, J.P., (2011), 'Toward a Standardized Thermal-Optical Protocol for Measuring Atmospheric Organic and Elemental Carbon: The EUSAAR protocol', Atmospheric Measurement Techniques, (3), 79–89.

Diapouli, E., Kalogridis, A.-C., Markantonaki, C., Vratolis, S., Fetfatzis, P., Colombi, C., Eleftheriadis, K. (2017), Annual Variability of Black Carbon Concentrations Originating from Biomass and Fossil Fuel Combustion for the Suburban Aerosol in Athens, Greece. Atmosphere, , 8, 234. https://doi.org/10.3390/atmos8120234.

EMEP/EEA air pollutant emission inventory guidebook 2019. European Environment Agency (http://efdb.apps.eea.europa.eu/) accessed 24 April 2023.

EEA Technical report No 18/2013, Status of black carbon monitoring in ambient air in Europe. Luxembourg: Publications Office of the European Union, 2013, ISBN 978-92-9213-415-0, ISSN 1725-2237, doi:10.2800/10150.

Gerlos-Nijland, M., Lanki, T., Salonen, R., Cassee, F. (2012), Health Effects of Black Carbon, Bonn: WHO Regional Office for Europe, The WHO European Centre for Environment and Health. ISBN: 9789289002653.

Hutzenberger R., Petzold A., Bauer H., Ctyroky P, Pouresmaeil P., Laskus, Puxbaum H., (2006), Intercomparison of Thermal and Optical Measurement Methods for Elemental Carbon and Black Carbon at an Urban Location Environ. Sci. Technol., 40, 6377-6383

Hristova, E., Veleva, B., (2020), Estimation of black carbon concentration in fine particulate matter in urban area. In Proceedings of the 20th International Multidisciplinary Scientific GeoConference SGEM 2020, Albena, Bulgaria, 16–25 August ; 20, 415-422.

Hristova, E., Georgieva, E.,Veleva, B., Neykova, N., Naydenova, S., Gonsalvesh-Musakova, L., Neykova, R., Petrov, A. (2022), Black Carbon in Bulgaria—Observed and Modelled Concentrations in Two Cities for Two Months. Atmosphere, 13, 213, https://doi.org/10.3390/atmos13020213.

IPCC. Climate change 2013: the physical science basis ; Working Group WG I contribution to the Fifth Assessment Report of the Intergovernmental Panel on Climate Change IPCC. 1535 (2014). ISBN 978-92-9169-138-8.

Kucbel M., Corsaro A., Švédová B., Raclavská H., Raclavský K., Juchelková D., (2017) Temporal and seasonal variations of black carbon in a highly polluted European city: Apportionment of potential sources and the effect of meteorological conditions. J. Environ. Manag., 203, 1178–1189.

Kunder R. D., Schneidemesser E., Kuik F., Quedenau J., Weatherhead E. C., Schmale J., (2018), Long-term monitoring of black carbon across Germany, Atmospheric Environment, 185, 41–52.

Petzold A., Ogren J.A., Fiebig M., Laj P., Li S.-M., Baltensperger U., Holzer-Popp T., Kinne S., Pappalardo G., Sugimoto N., Wehrli C., Wiedensohler A., Zhang X.-Y. (2013), Recommendations for reporting “black carbon” measurements. Atmos. Chem. Phys., 13, 8365–8379. https://doi.org/10.5194/acp-13-8365-2013.

Putaud J.-P., Van Dingenen R., Alastuey A., Bauer H., Birmili W., Cyrys J., Flentje H., Fuzzi S., Gehrig R., Hansson et al. (2010) A European aerosol phenomenology 3: Physical and chemical characteristics of particulate matter from 60 rural, urban, and kerbside sites across Europe. Atmo. Environ., 44, 1308-1320.

Slowik J. G.; Cross E. S.; Han J.-H.; Davidovits P.; Onasch T. B.; Jayne J. T.; Williams L. R.; Canagaratna M. R.; Worsnop D. R.; Chakrabarty R. K.; Muller H., Arnott W. P.; Schwarz J. P.; Gao Ru-S.; Fahey D. W.; Kok G. L.; Petzold A.. (2007), An Inter-Comparison of Instruments Measuring Black Carbon Content of Soot Particles, Aerosol Science and Technology, 41:295–314, 2007, ISSN: 0278-6826 print / 1521-7388 online, DOI: 10.1080/02786820701197078.

WHO global air quality guidelines. (2012) Particulate matter (PM2.5 and PM10), ozone, nitrogen dioxide, sulfur dioxide and carbon monoxide. Geneva: World Health Organization; Licence: CC BY-NC-SA 3.0 IGO.

Yttri K. E., Aas W., Bjerke A., Cape J. N., Cavalli F., Ceburnis D., Dye C., Emblico L., Facchini M. C., Forster C., Hanssen J. E., Hansson H. C., Jennings S. G., Maenhaut W., Putaud J. P., Tørseth K. (2007) Elemental and organic carbon in PM10: a one year measurement campaign within the European Monitoring and Evaluation Programme EMEP, Atmos. Chem. Phys., 7, 5711–5725, https://doi.org/10.5194/acp-7-5711-2007.

Zioła N., Błaszczak B., Klejnowski K. (2021) Long-Term eBC Measurements with the Use of MAAP in the Polluted Urban Atmosphere (Poland). Atmosphere, 12, 808. https://doi.org/10.3390/atmos12070808.